Pore Structure of Carbon−Mineral Nanocomposites and Derived Carbons Obtained by Template Carbonization

Teresa J. Bandosz, Jacek Jagiełło,† Karol Putyera,‡ and James A. Schwarz*

Department of Chemical Engineering and Materials Science, Syracuse University, Syracuse, New York 13244-1190

Received April 15, 1996. Revised Manuscript Received June 25, 1996[⊗]

The lithium form of taeniolite, intercalated with hydroxyaluminum and hydroxyaluminum−zirconium cations, served as the molecular template for carbon−mineral nanocomposites and derived carbons. The inorganic matrixes were saturated by furfuryl alcohol followed by its interlayer polymerization and carbonization. Carbons were derived after removal of the inorganic matrix. The surface and structural characteristics were obtained by X-ray diffraction, SEM, IGC, and sorption experiments (sorption of nitrogen, CH_4, CF_4, and SF_6). The results demonstrated that structural properties of the derived materials depend on the water content of the inorganic matrix. Molecular sieving properties of template derived carbons were also observed.

Introduction

The need for microporous materials with unique separation and storage properties has resulted in a search for either new methods of modification of sorbents or creation of new sources for such materials. One method that leads to the production of porous nanocomposites and/or carbons has been recently developed using the intracrystalline space of layered minerals for in situ carbonization.[1−4] Previously, template carbonization in the absence of water was used to obtain nonporous thin carbon films.[5−9] In our approach the properties of mineral matrixes as well as the nature of the organic precursor are used as experimental variables that can affect the porous properties of the final products. Specifically, using different inorganic matrixes can influence the microstructure of the materials derived because water, which is a natural component of the minerals, acts as a pore former during in situ carbonization/activation of organic material/carbonaceous deposit.[3,4] Its release provides the possibility of creating materials (carbon−mineral nanocomposites and derived carbons) for application in separation/storage systems where the size of pores is a critical factor. This is due to the fact that the limited thickness of carbon layers incorporated into the structures of the template prevents the creation of pores larger than the intercrystalline size.

The objective of this paper is to characterize the nanostructural properties of materials obtained from a synthetic mineral with a layered framework, taeniolite. Taeniolite has a chemical composition different from smectite (lack of hydroxyls in the structure of the layers[10]). Thus the influence of the water content introduced in the form of pillars on the final properties of the materials (carbon−mineral nanocomposites and derived carbons) obtained can be studied. It has been reported previously[3,4] that the chemical composition and thermal behavior of the host−guest system influence the mechanism of in situ carbonization. These factors may determine the adsorption properties of the resulting carbon−mineral nanocomposites and template-derived carbons. To study the influence of the above factors, we have chosen three different matrixes characterized by various interlayer compositions. In this paper we characterize the matrix, the nanocomposites, and the carbon derived from the nanocomposite. The results demonstrate the "templating effect" of the host on the derived materials.

Experimental Section

Materials. A set of nanocomposites and carbon samples was prepared using the synthetic mineral, taeniolite, provided by Topy Ind. Co. (Japan). The lithium form of this mineral (TL-0) has the following chemical formula: $Li(Mg_2Li)(Si_4)O_{10}F_2{\cdot}nH_2O$.[10] The sample of the mineral obtained from the manufacturer was either used as TL-0 or intercalated with inorganic polycations from solutions of either Chlorhydrol (TL-1) or Rezal 36G (TL-2). The chemical formulas of Chlorhydrol and Rezal 36G given by the manufacturer (Reheis Chemical Co.) are $Al_2(OH)_5Cl{\cdot}2.5H_2O$ and $Al_{1.2}Zr_{0.3}Cl{\cdot}5H_2O$, respectively. Samples TL-0, TL-1, and TL-2 were saturated with an 80% solution of furfuryl alcohol (FA) in benzene for 3 days. Polymerization was carried out by heating the samples under a N_2 flow at 353 K for 24 h and then at 423 K for 6 h. The

† Permanent address: Department of Fuels and Energy, University of Mining and Metallurgy, 30-059 Krakow, Poland.

‡ Permanent address: Institute of Inorganic Chemistry, Slovak Academy of Sciences, 842 36 Bratislava, Slovakia.

* To whom correspondence should be addressed.

[⊗] Abstract published in *Advance ACS Abstracts,* August 1, 1996.

(1) Bandosz, T. J.; Jagiełło, J.; Amankwah, K. A. G.; Schwarz, J. A. *Clay Miner.* **1992**, *27*, 435.

(2) Bandosz, T. J.; Putyera, K.; Jagiełło, J.; Schwarz, J. A. *Microporous Mater.* **1993**, *1*, 73.

(3) Bandosz, T. J.; Gomez-Salazar, S.; Putyera, K.; Schwarz, J. A. *Microporous Mater.* **1994**, *3*, 177.

(4) Bandosz, T. J.; Jagiełło, J.; Putyera, K.; Schwarz, J. A. *Carbon* **1994**, *32*, 659.

(5) Oya, A.; Yasuda, H.; Otani, S.; Yamada, Y. *J. Mater. Sci.* **1986**, *21*, 4481.

(6) Oya, A.; Sato, A.; Hanaoka, H.; Otani, S. *J. Am. Ceram. Soc.* **1990**, *73*, 689.

(7) Seron, A.; Ben-Maimoun, I.; Crispin, M.; Beguin, F. *Mater. Sci. Eng.* **1993**, *A168*, 239.

(8) Sonobe, N.; Kyotani, T.; Tomita, A. *Carbon* **1990**, *28*, 483.

(9) Kyotani, T.; Yamada, H.; Sonobe, N.; Tomita, A. *Carbon* **1994**, *32*, 627.

(10) Shell, H. R.; Ivey, K. H. *Bulletin 647*, U.S. Department of the Interior, Bureau of Mines, 1969.

S0897-4756(96)00233-5 CCC: $12.00

Scheme 1. Preparation of Materials

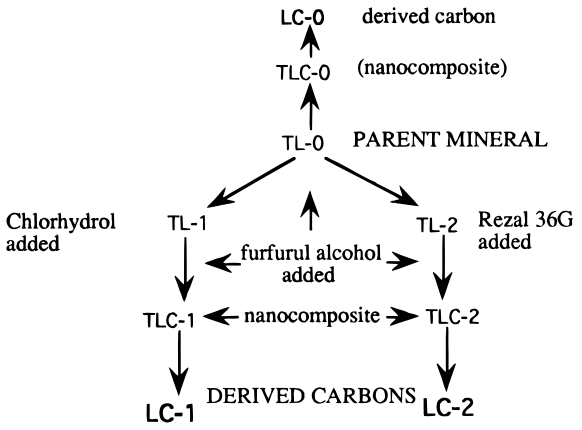

samples, with incorporated polymer in the interlayer space were heated at 973 K for 3 h under N_2 flow to carbonize the organic compound.[4,11,12] The carbon−mineral nanocomposites were designated as TLC-0, TLC-1, and TLC-2 depending upon the matrix used. The inorganic matrix was removed by extraction with hydrochloric and hydrofluoric acids and the resulting carbons obtained from taeniolite matrixes were designated as LC-0, LC-1, and LC-2 depending on the constitution of the matrix. Scheme 1 summarizes the inventory of materials that were derived from the parent mineral.

Methods. *X-ray Diffraction Analysis.* Taeniolite and carbon−mineral nanocomposite mounts were rehydrated at humidity below 50%. X-ray diffractograms were obtained with a Philips PW 1729 diffractometer using filtered Cu Kα radiation.

Scanning Electron Microscopy. Morphological observations were made with a scanning electron microscope (SEM) JEOL JSM-35G, operated at 24 kV after samples were coated in a Hummer II apparatus using Au−Pd electrodes.

Carbon Content. The carbon content was estimated by burning the organic deposit in the oven at 1273 K.

Inverse Gas Chromatography. Inverse gas chromatography experiments were conducted at infinite dilution. Detailed description of the method and derived parameters are given elsewhere.[13,14] Briefly, the thermodynamic parameters characterizing gas−solid interactions are obtained from the basic quantity measured in gas chromatography, the net retention volume, V_N.[15,16] It is related to the standard free energy of adsorption, ΔG, by the equation

$$\Delta G^\circ = -RT \ln \frac{V_N}{Sm} + C \qquad (1)$$

where R, T, m, and S are the gas constant, temperature, mass, and specific surface area of the adsorbent, respectively; C is a constant related to the standard state of gas and adsorbed phases. The ΔG is related only to gas−solid interactions since, under the conditions of infinite dilution, interactions between adsorbed molecules can be neglected.[13,15,16]

The chromatographic results were obtained for carbon samples (LC-1, LC-2) using an Antek 3000 gas chromatograph. Stainless steel columns 20 cm long and 2.17 mm in diameter were used. The experiments were performed at different temperatures between 573 and 673 K. Granulation of carbons was 0.2−0.4 mm. Before the experiments, the samples were conditioned at 673 K for 15 h under helium flow that was used as a carrier gas.

Table 1. X-ray Diffraction Results and Carbon Content

sample	d_{001} [Å]	gallery size [Å]	carbon content [%]
TL-0	12.1	2.1	
TL-1	18.8	8.8	
TL-2	18.2	8.2	
TLC-0	11.8	1.8	15
TLC-1	16.7	6.7	46
TLC-2	16.5	6.5	30
LC-1			80
LC-2			78

Branched alkanes (2,2-dimethylalkanes and 2-methylalkanes) in conjunction with *n*-alkanes were used as molecular probes.[3,11,14,17] They represent systematic structural changes and their critical sizes range from 3.6 Å (*n*-alkanes) to 4 Å (2-methylalkanes) to 6 Å (2,2-dimethylalkanes).[18] Quantities referenced to 2-methylalkanes and 2,2-dimethylalkanes adsorbates are denoted in the text by superscripts ′, and ″, respectively.

Sorption Experiments. Nitrogen isotherms were measured by a Gemini III 2375 surface area analyzer (inorganic matrixes and carbon−mineral nanocomposites) and ASAP 2000 (derived carbons, Micromeritics) at 77 K. Before the experiment the samples were heated for 10 h at 473 K and then outgassed at this temperature under a vacuum of 10^{-2} mmHg. The isotherms were used to calculate the specific surface area, micropore volume (DR)[19] and pore size distributions (PSDs) using density functional theory (DFT).[20]

Methane, carbon tetrafluoride, and sulfur hexafluoride adsorption isotherms were measured on the Gemini III 2375. The pretreatment of the samples was the same as in the case of nitrogen adsorption and the isotherms were measured around room temperature (about 250, 270, and 290 K). The apparatus was equipped with a homemade thermostated system controlled by a Fisher Scientific Isotemp Refrigerated Circulator, Model 900. From the adsorption isotherms the heats of adsorption were calculated.[21−23]

Results and Discussion

The results of the X-ray diffraction study show a significant increase in the d_{001} parameter of taeniolite after its intercalation with inorganic polycations. The values collected in Table 1 are similar to those obtained for intercalated montmorillonites.[1,24−28] The d_{001} values obtained are considered here as average ones due to some inhomogeneity in the structure. Data presented in Table 1 indicate the average height of the introduced pillars which is equal to the gallery size (spacing). The average value of the spacing obtained for the sample intercalated with Chlorhydrol is 8.8 Å. This value is in agreement with the size of hydroxyaluminum Al_{13}

(11) Bandosz, T. J.; Jagiełło, J.; Putyera, K.; Schwarz, J. A. *Langmuir* **1995**, *11*, 3964.
(12) Bandosz, T. J.; Jagiełło, J.; Putyera, K.; Schwarz, J. A. *Clays Clay Miner.* **1996**, *44*, 237.
(13) Jagiełło, J.; Bandosz, T. J.; Schwarz, J. A. *J. Colloid Interface Sci.* **1992**, *151*, 433.
(14) Jagiełło, J.; Bandosz, T. J.; Schwarz, J. A. *Carbon* **1992**, *30*, 63.
(15) Kiselev, A. V.; Yashin, Y. I. *Gas Adsorption Chromatography*; Plenum: New York, 1969.
(16) Conder, J. R.; Young, L. C. *Physical Measurements by Gas Chromatography*; Wiley: New York, 1979.
(17) Jagiełło, J.; Bandosz, T. J.; Putyera, K.; Schwarz, J. A. In *Characterization of Porous Solids-III*; Rouquerol, J., Rodrigez-Reinoso, F., Sing, K. S. W., Unger, K. K., Eds.; Elsevier: Amsterdam, 1994; p 679.
(18) Roberts, R. A.; Sing, K. S. W.; Tripathi, V. *Langmuir* **1987**, *3*, 331.
(19) Dubinin, M. M. In *Chemistry and Physics of Carbon*; Walker, P. L., Jr., Ed.; Marcel Dekker: New York, 1966; Vol. 2.
(20) Olivier, J. P.; Conklin, W. B. *Presented at 7th Int. Conf. Surf. Colloid Sci.*, Compiegne, France, 1991.
(21) Jagiełło, J.; Schwarz, J. A. *Langmuir* **1993**, *9*, 2513.
(22) Jagiełło, J.; Bandosz, T. J.; Putyera, K.; Schwarz, J. A. *J. Chem. Soc., Faraday Trans.* **1995**, *91*, 2929.
(23) Putyera, K.; Jagiełło, J.; Bandosz, T. J.; Schwarz, J. A. *Carbon* **1995**, *33*, 1047.
(24) Occelli, M. L.; Tindwa, P. M. *Clays Clay Miner.* **1983**, *31*, 22.
(25) Pinnavaia, T. J. *Science* **1983**, *220*, 365−371.
(26) Bandosz, T. *Bull. Pol. Acad. Sci.: Chem.* **1991**, *39*, 167.
(27) Baksh, M. S. A.; Yang, R. T. *AIChE J.* **1992**, *38*, 1357.
(28) Gil, A.; Montes, M. *Langmuir* **1994**, *10*, 291.

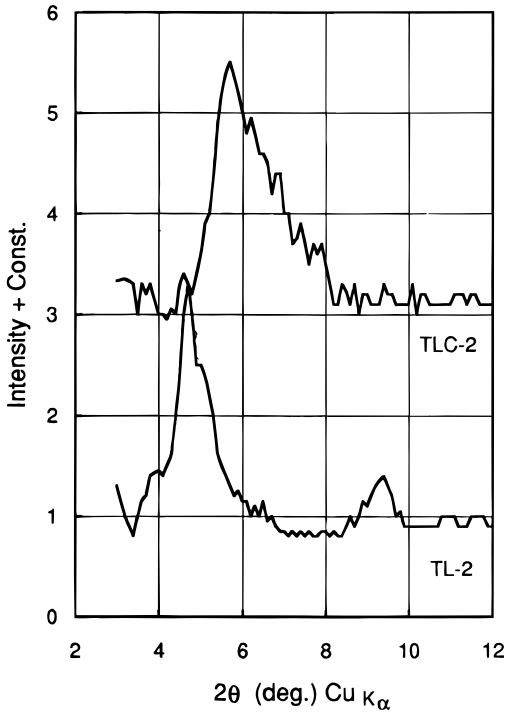

Figure 1. X-ray diffraction pattern for TL-2 and TLC-2 samples.

Keggin polycations,[29] which are likely present between the mineral layers.[24,29] The sample intercalated with Rezal 36G is characterized by pillars of a smaller size. Their structure is not well defined. More than a factor of 2 greater cation exchange capacity (CEC) of taeniolite (260 mequiv/100 g[30]) compared to smectite suggests a much higher density of pillars in the former. As a basis for comparison, according to Winans and Cerrado, Al_{13} pillars in smectite are separated on the average by 14 Å.[31]

It is interesting to note that the intercalated taeniolites saturated with poly(furfuryl alcohol) withstood heat treatment to 973 K without the collapse of their layered framework and well-defined d_{001} peaks are observed (Figure 1). Their d_{001} parameters decreased from 18.2−18.8 Å to about 16.5 Å after heat treatment, which is probably limited by the thickness of the carbon deposit present between the layers.[2−4] The thickness of the carbon deposit is calculated subtracting the thickness of mineral layers from the value of d_{001} parameter. Taking into account the broadness of diffraction peaks obtained for nanocomposites (Figure 1), indicating some degree of structural heterogeneity this quantity is considered as an average.

The carbonization temperature, chosen to be 973 K, is in the temperature range where the simultaneous dehydroxylation of the intercalated polycations is also occurring.[3,4] This coincidence of dehydroxylation and carbonization during template carbonization can be significant in the process of pore formation[3,4,9] due to the fact that water released from the structure of the matrix can act as a pore former or "activation" agent. Within the nanodimensional confines of the rigid mineral structure, the generation of water vapor at extremely high pressure can create fine microporosity by mechanisms similar to those occurring during conventional steam activation of carbonaceous chars. On the basis of the chemical formulas of intercalating compounds we estimate that hydroxycations derived from Rezal 36G (hydroxyaluminum−zirconium polycations) have about 20% less chemically bound water than species present in Chlorhydrol (hydroxyaluminum polycations). This is due to the fact that in the case of Chlorhydrol, besides water of hydration, OH groups also contribute in generation of water vapor at high temperature. Since dehydroxylation occurs at higher temperature than dehydration it may suggest that water from OH groups of hydroxycations is more active in the process of pore creation. The above suggests that carbon obtained from the TL-2 (taeniolite intercalated with hydroxyaluminum−zirconium polycation) matrix, LC-2, should have smaller pores than its counterpart obtained in the TL-1 matrix (taeniolite intercalated with hydroxyaluminum polycation), LC-1. On the other hand, oxide species or metalocations,[24] present within the structure after dehydroxylation and then removed by acid washing can also contribute in the development of porosity.[31] At this stage of our understanding, it is difficult to draw any conclusion about the size of oxide clusters. Although the initial average sizes of hydroxymetallic polycations are similar to each other (Table 1), their thermal stability is different,[32] which may also affect the final sizes of oxide pillars and hence the size of the voids left after removal by acid.

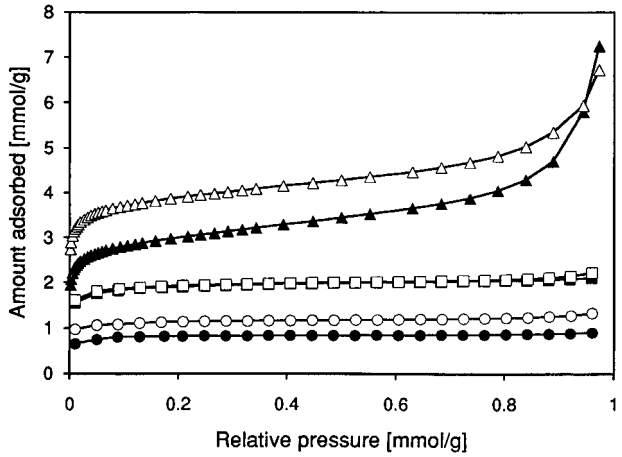

Figure 2. Nitrogen adsorption isotherms at 77 K. □, TL-1; ○, TL-2; ■, TLC-1; ●, TLC-2; △, LC-1; ▲, LC-2.

Differences in nitrogen adsorption isotherms presented in Figure 2 reflect variations in samples' pore structure. Isotherms obtained for the intercalated taeniolites (TL-1 and TL-2) and carbon-taeniolite nanocomposites (TLC-1 and TLC-2) are typical type I Langmuir shaped isotherms characteristic of microporous solids. Differences in the sorption uptake of the samples intercalated with Chlorhydrol (hydroxyaluminum polycations), TL-1 and Rezal 36G (hydroxyaluminum−zirconium polycations), TL-2, are related to a smaller gallery size for the latter sample. It is also likely that different spatial arrangement of polycation species between the layers could result in differences in adsorp-

(29) Plee, D.; Borg, F.; Gatineau, L.; Fripiat, J. J. *J. Am. Chem. Soc.* **1985**, *107*, 2362.
(30) Bandosz, T. J.; Putyera, K.; Jagiełło, J.; Schwarz, J. A.; Rouzaud, J.-N.; Beguin, F.; Ben-Maimoun, I. *J. Chem. Soc., Faraday Trans.* **1995**, *91*, 493.
(31) Winans, R. E.; Carrado, K. A. *J. Power Sources* **1995**, *54*, 11.
(32) Bandosz, T. J.; Jagiełło, J.; Schwarz, J. A. *J. Phys. Chem.* **1995**, *99*, 13522.

Table 2. Structural Parameters Calculated from Nitrogen Sorption Isotherms[a]

sample	S_{N_2} [m²/g]	V_{mic} [cm³/g]	V^*_{mic} [cm³/g]	S_{mic} [%]
TL-0	2			
TL-1	182	0.056		83
TL-2	115	0.031		77
TLC-0	2			
LC-0	146	0.010		
TLC-1	193	0.060		88
LC-1	460	0.120	0.092	66
TLC-2	83	0.030		86
LC-2	330	0.070	0.050	71

[a] S_{N_2}, specific surface area; V_{mic}, micropore volume calculated using the DR method; V^*_{mic}, volume in pores smaller than 11.78 Å; S_{mic}, percentage of surface area in micropores.

tion properties. Similar gallery size for both TL-1 and TL-2 suggests that in the case of the TL-2 sample pillars are arranged within the interlayer space more densely compared to the TL-1 sample and penetration of a nitrogen molecule is restricted. Incorporation of carbon does not significantly change the microporous nature of the solids. The almost unchanged shape of the isotherms for TL-1 and TLC-1 samples which leads to similar structural characteristics appears to be the result of compensating factors. At this stage of our understanding we can only speculate on the nature of the complex processes occurring within the interlayer space during polymerization/carbonization. In the case of taeniolite with hydroxyaluminum pillars we previously observed a significant increase in the surface area and porosity caused by heat treatment at 673 K related to loss of water and opening more interlayer space for nitrogen adsorption.[32] This process may be accompanied by expansion of the carbon deposit resulting in the creation of more pores. We propose that the effects of the filling of the interlayer space with organic deposit along with expansion of the carbon layer in the horizontal direction, and pore creation due to the presence of water are responsible for the overall unchanged sorption characteristic of these two materials. A decrease in the sorption uptake for the TLC-2 sample compared to TL-2 is related to lower porosity created within the carbonaceous deposit compared to the TLC-1 sample. These phenomena could be due to either differences in the water content or thermal stability of hydroxyaluminum−zirconium species when compared to hydroxyaluminum ones.[32]

When the isotherms for template-derived carbons are considered, their shape indicates significant changes in the porous nature of these materials. The initial part of the isotherms still retains its Langmuir shape. Their higher adsorption uptake at low relative pressure compared to the matrix and nanocomposite counterparts indicates a significant contribution of micropores to the total porosity of the carbons. When the relative pressure increases, sorption in larger pores plays a role. The observed shape of the isotherms for template-derived carbons can be explained by the presence of mesopores which are created between the small carbon particles removed from the matrix.

Analysis of the results of nitrogen adsorption experiments provides basic information about the pore structure of all samples. The calculated adsorption parameters: specific surface area (S_{N_2}), micropore volumes (V_{mic}) and percentage of surface area in micropores (S_{mic}) are collected in Table 2. The surface areas for the set

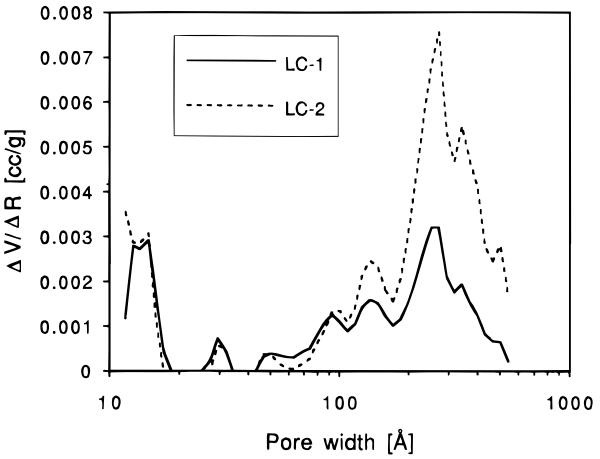

Figure 3. Pore size distributions for LC-1 and LC-2 carbons.

of carbon−mineral nanocomposites decrease in the order TLC-1, TLC-2, TLC-0. The dependence obtained was expected, and it agrees with the decreasing water content in the samples studied; in the case of TLC-1 and TLC-2, water (as a pore former) was introduced during the process of intercalation as a constituent of the pillars. In these cases, similar to that of smectites,[3,4] samples obtained from the matrix intercalated with Chlorhydrol (hydroxyaluminum pillars) have higher surface area due to the fact that larger pores could be created (more water was released). In the case of samples derived from lithium taeniolite as a host (TLC-0), a nonporous surface was obtained due to the lack of any pore former.[30]

The carbons obtained from intercalated matrixes are characterized by surface areas of about 400 m²/g and micropore volumes of about 0.100 cm³/g (Table 2). The specific surface areas and micropore volumes decrease in the same order as was observed for the parent carbon−mineral nanocomposites (LC-1, LC-2, LC-0). This ordering is in agreement with that of a previous study.[4] We propose that water released during simultaneous dehydroxylation/carbonization is a pore former for the carbonaceous deposit present between the mineral layers. It can create small pores whose sizes depend on the extent of water available and the thickness of the carbon deposit. Both factors are responsible for the subtle differences in the microstructures of the final materials.

The distribution curves for the microporous carbons calculated using density functional theory (DFT)[20] are collected in Figure 3; due to the limit of our experimental pressure pores smaller than 11.78 Å are not reported. In the range of pores having radii between 11.78 and 100 Å, the PSDs obtained are very similar to each other. In the case of the LC-2 sample the high contribution of large intercrystalline pores is observed. The differences in porosity are probably related to the different spatial arrangement of carbon crystallites extracted from the matrixes. Using DFT, one can estimate the volume in very small pores outside the applied experimental range. The total volume in pores of ≤11.78 Å is reported in Table 2 as V^*_{mic}. Analysis of these values in comparison with total micropore volumes calculated using the Dubinin−Radushkevich (DR) method based on theory of volume filling of micropores (TVFM)[19] indicates that the majority of micropore volumes is in supermicropores ≤11.78 Å (over 70%),

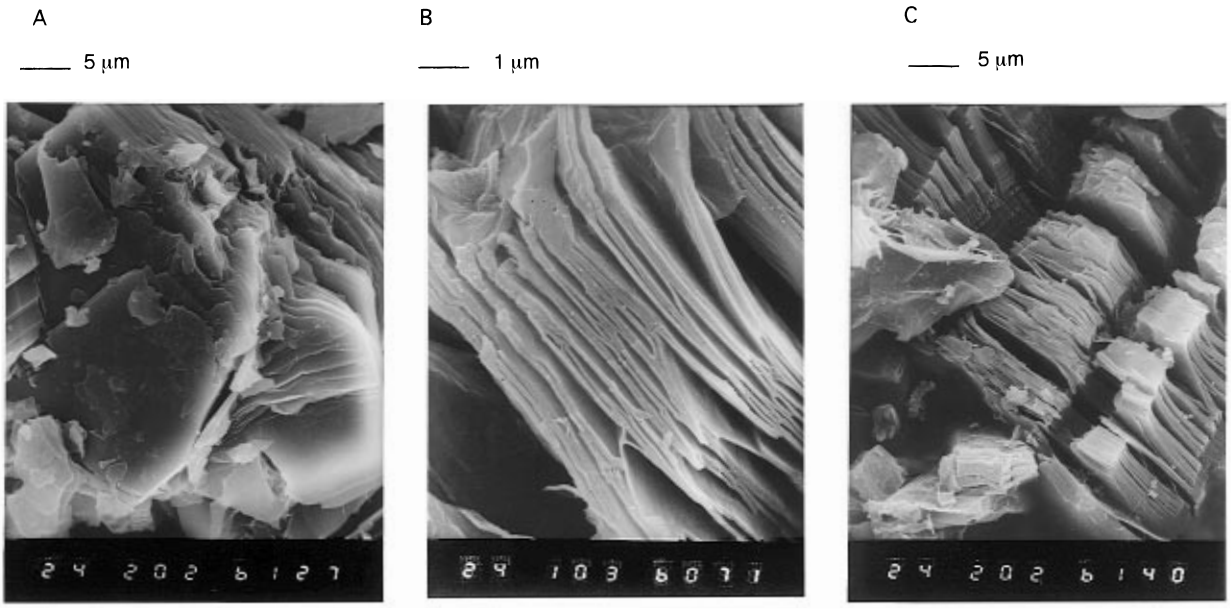

Figure 4. SEM micrographs of the TL-0 (A), TLC-1 (B), and LC-1 (C) samples.

which can be created in the thin carbon deposit within the interlayer space.

In our interpretation of the process of pore creation, we do not exclude the contribution of the different shapes of pillars; however, our hypothesis of the dominant role of water released from hydroxycations is based on systematic sorption studies of matrixes, nanocomposites, and carbon. The observed smaller surface area and micropore volume accompanied with almost the same interlayer space for the TL-2 matrix compared to TL-1 may indicate a higher density of pillars for the former. If pores in our carbon deposit are only the result of the presence of pillars in "the negative image", after the removal of the inorganic matrix, the micropore volume of the LC-2 carbon should be higher compare to the LC-1 carbon. What is observed is opposite: the LC-1 carbon has almost a factor of 2 higher micropore volume compared to LC-2. A similar relationship is observed for TLC-1 nanocomposite compared to TLC-2. This indicates the "memory effect" of the matrix on the properties of extracted carbons. The above observation supports our hypothesis of the dominant role of water in the process of pore creation in carbon deposits within the structure of pillared clays.

The surface topography of the carbon−mineral nanocomposites and carbons has been analyzed by scanning electron microscopy. Figure 4A is the SEM micrograph of the initial lithium form of taeniolite (TL-0); thin silicate layers are clearly seen. In the case of the TLC-1 sample (Figure 4B) the layered framework of the inorganic precursor is preserved; however, the silicate layers become more separated from each other, forming a more open structure. The material appears to be uniform and a separated phase of amorphous carbonaceous material cannot be seen. Thus, all carbon (~50% of sample weight) is probably incorporated within the interlayer space. After removal of the inorganic matrix, the LC-1 carbon is also characterized by a highly organized layered structure similar to its original parent mineral and carbon−mineral nanocomposite (Figure 4C).

Analysis of the total sorption capacity of CH_4, CF_4, and SF_6 at a pressure of 760 mmHg provides additional

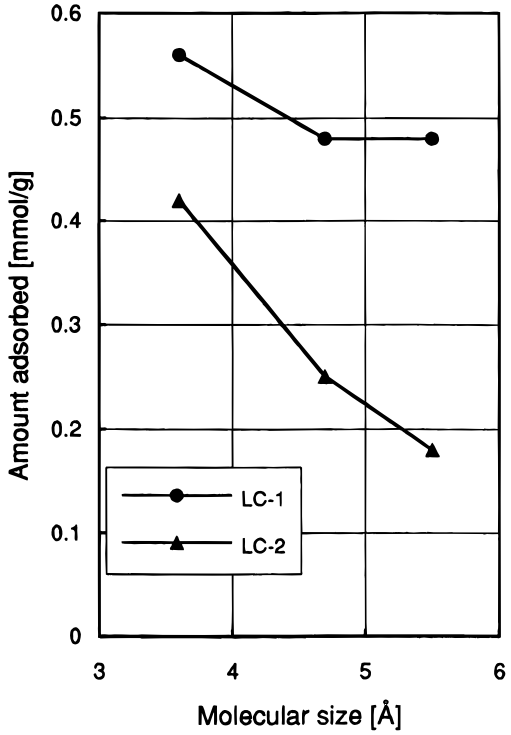

Figure 5. Dependence of amount adsorbed versus molecular size of the adsorbate (297 K, 760 mmHg). Sizes of probe molecules: CH_4 3.6 Å, CF_4 4.6 Å, SF_6 5.5 Å.

structural information. The total uptake for the LC-1 and LC-2 carbons decreases with an increase in the molecular size of the sorbate. This decrease is probably due to the fact that not all pores accessible for methane are accessible for either carbon tetrafluoride or sulfur hexafluoride.

The phenomena observed indicate the sieving properties of the carbons which, under certain conditions, can be used to separate small gas molecules. In Figure 5 we present the relationship of the total amount adsorbed (297.5 K, 760 mmHg) versus the size of the adsorbate. In both cases, a decrease compared to the methane sorption capacity is observed. This decrease is the most

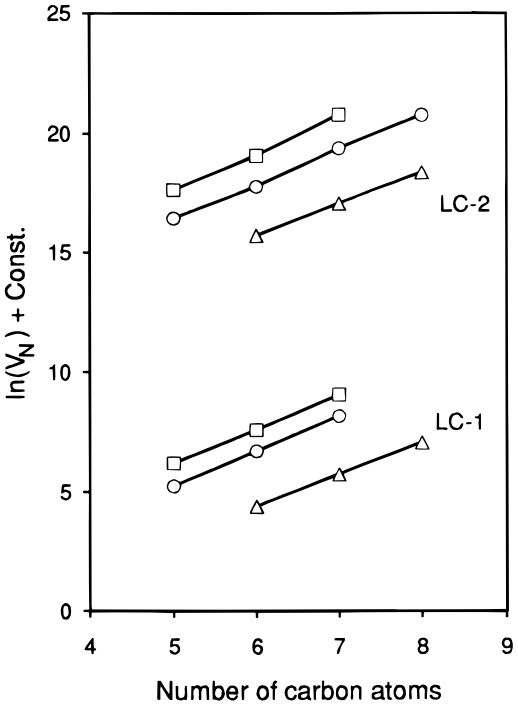

Figure 6. Variation of the net retention volumes of *n*-alkanes (□), 2-methylalkanes (○), 2,2-dimethylalkanes (△) measured at 573 K, versus their number of carbon atoms.

Table 3. IGC Results at 578 K[a]

sample	$-\Delta G_{CH_2}$ [kJ/mol]	$-\Delta G'_{CH_2}$ [kJ/mol]	$-\Delta G''_{CH_2}$ [kJ/mol]	$-\Delta'$	$-\Delta''$	S' [%]	S'' [%]
LC-1	6.8	7.0	6.4	0.88	3.27	35	91
LC-2	7.0	6.5	6.3	1.35	3.53	59	93

[a] $-\Delta G_{CH_2}$, free energy of adsorption of one CH_2 segment in alkane molecule; $-\Delta G'_{CH_2}$, free energy of adsorption of one CH_2 segment in 2-methylalkane molecule; $-\Delta G''_{CH_2}$, free energy of adsorption of one CH_2 segment in 2,2-dimethylalkane molecule; Δ', shift between $\ln(V_N)$ of alkanes and 2-methylalkanes; Δ'', shift between $\ln(V_N)$ of alkanes and 2,2-dimethylalkanes; S', percentage of surface area in pores inaccessible for 2-methylalkanes; S'', percentage of surface area in pores inaccessible for 2,2-dimethylalkanes.

pronounced in the case of the LC-2 sample; here, the smallest pores are created due to the lower water content of the matrix.[3]

To further confirm the existence of sieving properties for small molecules, we performed an inverse gas chromatography study at infinite dilution. The results obtained are presented in Figure 6. The free energies of interaction of one CH_2 segment of the alkane, $\Delta G(CH_2)$ (slopes of the lines), are collected in Table 3. High values indicate the presence of small pores.[13] Table 3 also contains the average shift of branched isomer lines from their corresponding parent alkane line. They are denoted as Δ' and Δ'' for 2-methylalkanes and 2,2-dimethylalkanes, respectively. The shift of $\ln(V_N)$ lines for the isomers is due to the fact that part of the branched molecule cannot be accommodated in the same plane parallel to the surface, and the total contribution to the interaction energy of the branched molecule is smaller than that of the more flexible *n*-alkane molecules.[33] When microporous materials that contain pores not accessible for branched molecules are considered, an additional shift in the $\ln(V_N)$ lines occurs since V_N is proportional to the accessible surface or number of adsorption sites (see eq 1). A similar approach which resulted in defining a morphology index was described independently by Balard and Papirer.[34]

Table 4. Isosteric Heats of Adsorption at Zero Surface Coverage

sample	$Q^{\circ}_{st}(CH_4)$ [kJ/mol]	$Q^{\circ}_{st}(CF_4)$ [kJ/mol]	$Q^{\circ}_{st}(SF_4)$ [kJ/mol]
LC-1	22.5	24.2	34.0
LC-2	22.7	24.8	37.9

We have previously reported the analysis of data obtained on a nonporous carbon considered as a reference material.[17,33] In the case of that carbon the shift of $\ln(V_N)$ occurs only due to different spatial orientations of the alkane molecule. The Δ' and Δ'' values obtained on that reference carbon, at the temperature used in this work (573 K), were 0.45 and 0.80, respectively. Taking the difference in Δ' and Δ'' values for the porous carbons and a nonporous reference, we can calculate the percentage of surface excluded as a result of sieving effects. For instance, in the case of the LC-2 carbon $\Delta\ln(V_N)$ is 2.73, reflecting a net effect due to exclusion of a certain number of adsorption sites in the pores. From eq 1 we calculate that the number of adsorption sites accessible for 2,2-dimethylalkanes is about 15 times smaller when compared with the surface accessible for the *n*-alkane. Taking into account the critical size of 2,2-dimethylalkane, 0.6 nm,[18] and the size of the alkane, 0.36 nm, we find that, in the case of the LC-2 sample, about 93% of the surface accessible for the *n*-alkane is not accessible for 2,2-dimethylalkane because the surface is confined to pores in the range up to 0.6 nm. The same calculation considering the 2-methylalkane molecule reveals that only 59% of surface accessible for hexane is inaccessible for 2-methylpentane. The surface exclusions calculated in this way are collected in Table 3. Once again it is seen that the highest contribution of smallest pores is present in the structure of the LC-2 carbon. It is noted that in the case of our template-derived carbons the contribution of surface in small pores is twice as great as that obtained for the commercial molecular sieving carbon, Carbosieve G.[33]

Self-consistency is provided by the relationship between the isosteric heats of adsorption; they are also related to the pore size distribution. The isosteric heats of adsorption of CH_4, CF_4, and SF_6 at zero surface coverage are collected in Table 4. Under these conditions gas−gas contributions to interaction energies and isosteric heats are minimized. The smallest pores in the case of LC-2 carbon enhance the adsorption energy; in all cases Q°_{st} are higher for this carbon compared to the corresponding values obtained on the LC-1 sample.

Conclusion

Synthesis of materials within matrixes of nanometer dimensions critically depend on the properties of the matrix. It was shown that even when the same organic precursor is used, small differences in the water content and chemical compositions of the matrixes are crucial for the micropore structure development of sorbents. We demonstrate that by in situ carbonization of organic compounds one can obtain carbon−mineral nanocomposites and microporous carbons with a developed pore

(33) Jagiełło, J.; Bandosz, T. J.; Schwarz, J. A. *Carbon* **1994**, *32*, 687.
(34) Balard, H.; Papirer, E. *Prog. Org. Coat.* **1993**, *22*, 1.

structure and a high content of their surface area in micropores (about 90% of the total surface area in the case of nanocomposites and about 70% of the total surface area in the case of carbons). The carbons obtained are characterized by the presence of very small pores (about 80% of micropore volume is in pores smaller than 11.78 Å) which, under certain conditions, can separate molecules whose diameters differ by less than 1 Å. We propose that water released from pillars is the dominant factor in the process of pore creation in the carbon deposit. Complementary experiments such as DTG, IR, and SANS should bring new insight leading to a better understanding of the processes occurring within the interlayer space.

CM960233I